Dispersion of ultrasound by conduction electrons calculated from the deformation coefficient

J. D. Gavenda, C. M. Casteel,* and W. M. Theis†
Department of Physics, The University of Texas at Austin, Austin, Texas 78712
(Received 13 May 1982)

We extend Pippard's theory for ultrasonic attenuation in metals, based on a Fermi-surface deformation coefficient, to include the calculation of the dispersion. We make use of the transient-stress method developed by Kadanoff and Pippard for the case of zero applied field. The resulting expressions are applied to jellium, giving magnetic-field-dependent attenuation and dispersion with minimal restrictions on ql or $\omega\tau$ which agree with earlier semiclassical calculations carried out in the laboratory frame. We point out a striking reversal in the phase of oscillations in the sound velocity as a function of magnetic field intensity for shear waves when $\omega_c\tau \approx \pi$. Asymptotic analytic expressions are given for the attenuation and dispersion for $ql/\omega_c\tau > 4$.

I. INTRODUCTION

In a recent paper[1] by two of the present authors it was shown that calculations using Pippard's theory[2] for ultrasonic attenuation in metals, based on a Fermi-surface deformation coefficient, agreed rather well with measurements of open-orbit resonant attenuation in copper. This led us to attempt a similar comparison for variations in the velocity of sound as a function of applied magnetic field intensity.

Although many authors[3–7] have presented theories for ultrasonic dispersion, most of them are so general as to be difficult to use for numerical calculations, or else specialized to particular experimental conditions. We present here a general method for extending Pippard's theory for the attenuation to include the dispersion as well.

We find the attenuation and velocity shift to be proportional to the imaginary and real parts, respectively, of the transient stress defined by Kadanoff and Pippard[8] (KP). The transient stress is calculated from the deformation force plus a fictitious force caused by the use of a reference frame moving with the lattice and the self-consistent electric field required to screen out the currents caused by the first two forces.

In the following section we derive general expressions for attenuation and velocity shift as outlined above. In Sec. III we apply these expressions to the jellium model and show that our results agree with those obtained previously in the laboratory reference frame. Our results are somewhat more general in that the ranges of ql and $\omega\tau$ are not as restricted as in some of the earlier works. Here $\vec{q}$ is the wave vector and ω the frequency of the sound; l is the mean free path and τ the relaxation time of the electrons.

Asymptotic analytic expressions for the sound velocity and attenuation in the limit $D \gg \lambda$ are given in Sec. IV, where D is the extremal orbit diameter and λ the sound wavelength. These expressions reproduce the numerical calculations quite well for $D > 4\lambda$.

II. GENERAL THEORY FOR ATTENUATION AND DISPERSION OF ULTRASOUND

A. Derivation of the dispersion equation

We follow the notation of Landau and Lifshitz[9] in writing the acoustic-wave equation

$$\rho \ddot{u}_i = \frac{\partial \sigma_{ik}}{\partial x_k}, \qquad (1)$$

where ρ is the mass density of the metal and u_i is the lattice displacement. The stress tensor σ_{ik} is related to the free energy F by

$$\sigma_{ik} = \frac{\partial F}{\partial e_{ik}}, \qquad (2)$$

where e_{ik} is the acoustic strain $\partial u_i/\partial x_k$. The free energy is, in turn, related to the strain tensor by

$$F = \tfrac{1}{2}\lambda_{iklm} e_{ik} e_{lm}, \qquad (3)$$

where λ_{iklm} is the elastic-modulus tensor. We will assume that it includes both the elastic modulus of the lattice ions and the contributions from the equilibrium distribution of the conduction electrons. We further assume that a sudden deformation of the crystal leads to an additional contribution to the free energy caused by the nonequilibrium distribution of the electrons. This contribution is expressed in terms of the transient-stress tensor $\underline{T}$ discussed by

KP.

If we specialize to the case of an acoustic wave propagating along x so that the lattice displacement is given by $ue^{i(\omega t - qx)}$, Eq. (1) reduces to

$$i\rho\omega\dot{u} = -q^2\rho v_0^2 u - iqT \ , \qquad (4)$$

where v_0 is the sound velocity for this particular mode in the absence of the transient stress. Here T represents the component of the transient-stress tensor appropriate for the mode. We have assumed that T varies linearly with lattice displacement. Furthermore, any contributions of T to offdiagonal components of the elastic modulus are assumed to be neglected in order to simplify the calculations which follow. This approximation may not be valid in the presence of a magnetic field when the sound propagates along a crystal axis for which there are degenerate modes. The effect of the Lorentz force on ions moving in a magnetic field is assumed to be included in v_0 in Eq. (4).

We define $q_0 = \omega / v_0$ and rewrite Eq. (4) to obtain the dispersion equation in terms of the transient stress,

$$q^2 = q_0^2(1 + qT/\rho\dot{u}\omega) \ . \qquad (5)$$

The solution, to first order in $T/2\rho v_0 \dot{u}$, is

$$q = q_0(1 + T/2\rho v_0 \dot{u}) \ . \qquad (6)$$

If we take q to be complex, the attenuation α can be found from

$$\alpha = -2\,\mathrm{Im} q \ , \qquad (7)$$

and the sound velocity from

$$v_s = \omega / \mathrm{Re} q \ . \qquad (8)$$

In terms of the transient stress the relative attenuation is given by

$$\alpha / q_0 = -(\rho v_0)^{-1} \mathrm{Im}(T/\dot{u}) \ , \qquad (9)$$

and the fractional velocity shift by

$$\delta v_s / v_0 = -(2\rho v_0)^{-1} \mathrm{Re}(T/\dot{u}) \ , \qquad (10)$$

to first order in α / q_0 and $\delta v / v_0$.

B. Calculation of the transient stress

KP showed that the transient stress can be calculated from

$$T = -(4\pi^3)^{-1} \int D \, \Delta\epsilon \, dS \ , \qquad (11)$$

where D is the net shift of an electron's wave vector away from the Fermi surface per unit strain, and $\Delta\epsilon$ is the change in energy of the electron caused by the real and fictitious forces acting on it, which leads to a nonequilibrium distribution function.[10] In this derivation we will assume that the magnetic field is not large enough to introduce quantum effects.

A strain $\underset{\sim}{e}$ causes the Fermi surface to shift by an amount $\vec{K}\cdot\underset{\sim}{e}$ normal to itself, where $\vec{K}$ is the deformation coefficient. Since these calculations are carried out in a reference frame attached to the lattice, a dynamic strain also causes the electron wave vectors to change. The net shift of electron wave vector away from the Fermi surface is the sum of these contributions and is denoted by $-De$, where

$$D = (\vec{K} + \vec{k}\cos\phi)\cdot\hat{u} \ , \qquad (12)$$

and where ϕ denotes the angle between $\vec{q}$ and the electron velocity $\vec{v}$. This shift causes the electron to gain energy $-\hbar v D e$ with respect to the Fermi energy and thus to contribute $-\hbar v D$ to the stress.

The factor $\Delta\epsilon$ arises in Eq. (11) from taking into account the total number of electrons contributing to the stress. It is calculated by using Chambers's path-integral method,[11]

$$\Delta\epsilon(\vec{r}(t_0), \vec{k}(t_0)) = \int_{-\infty}^{t_0} dt \, Fv \exp\left[-\int_t^{t_0} dt/\tau \right] \ , \qquad (13)$$

where F is the net force along the path of the electron. The two forces which act on the electron are the fictitious force

$$\Pi = iq\hbar\dot{u}D \ , \qquad (14)$$

which represents the effect of deforming the Fermi surface, viewed from the moving lattice, and the self-consistent electric field force $e\vec{E}\cdot\hat{v}$, which acts to restore current neutrality in the strained lattice.

The field $\vec{E}$ is obtained by calculating the current $\vec{j}^{\,\mathrm{def}}$ which would arise from Π alone and finding the field necessary to screen it,

$$E_j = -\rho_{ij} J_i^{\mathrm{def}} \ , \qquad (15)$$

where ρ_{ij} are components of the resistivity tensor $\underset{\sim}{\rho}$. This assumption of perfect screening, valid for typical experimental conditions, is introduced to simplify the calculations. One could instead introduce Maxwell's equations via the tensor $\underset{\sim}{M}$ defined by Cohen, Harrison, and Harrison[12] (CHH) and replace $\underset{\sim}{\rho}$ by $(\underset{\sim}{\sigma} + \underset{\sim}{M})^{-1}$, where $\underset{\sim}{\sigma}$ is the conductivity tensor.

The deformation current is calculated from

$$\vec{J}^{\,\mathrm{def}} = \frac{e}{4\pi^3\hbar} \int \hat{v} \, \Delta\epsilon^{\mathrm{def}} dS \ , \qquad (16)$$

where $\Delta\epsilon^{\mathrm{def}}$ is found by using Π only in Eq. (13).

III. APPLICATION TO A FREE-ELECTRON METAL

Although the method outlined in the preceding section should be applicable to metals with arbitrarily shaped Fermi surfaces, it is instructive to apply it first to a free-electron metal, i.e., so-called "jellium." Pippard showed the equivalence between his calculation of attenuation, using the deformation coefficient in a reference frame moving with the lattice, and the laboratory-frame calculation of CHH for jellium, in the large-ql limit. We will extend the comparison to arbitrary ql and $\omega\tau$,[13] and calculate the velocity of sound as well.

The direction of propagation is taken along x and the applied magnetic field along z. We adopt Pippard's notation for the various polarization possibilities: case $(\vec{i},\vec{k})$, longitudinal waves, case $(\vec{j},\vec{k})$, transverse waves polarized along the y axis, and case $(\vec{k},\vec{k})$, transverse waves polarized along the z axis.

Since the forces which contribute to F in Eq. (13) are proportional to the lattice displacement, they must vary as $e^{i(\omega t-qx)}$; therefore Eq. (13) can be written as

$$\Delta\epsilon(\vec{r},\vec{k},0)=\int_{-\infty}^{0}dt'\,F_0 v\exp\left[-iqx'-\int_{t'}^{0}dt''\left[\frac{1+i\omega t}{\tau}\right]\right]. \tag{17}$$

Following Pippard, we transform the integrals over time to integrals along the path in $\vec{k}$ space,

$$\Delta\epsilon=\frac{\hbar}{eB}\int_{-\infty}^{s}ds'\,F_0\csc(\theta')\exp\left[-i\beta(k_y-k_y')+\int_{s}^{s'}ds''a\right], \tag{18}$$

where $\beta=\hbar q/eB$,

$$a=\beta(1+i\omega\tau)/(ql\sin\theta)\,,$$

and θ is the angle between $\vec{v}$ and $\vec{B}$. This is the same as Pippard's result following his Eq. (36) except that he neglected $\omega\tau$, since it is usually small for most experimental conditions. Since the electronically induced velocity shift turns out to be proportional to $\omega\tau$, we must not neglect it. Equation (18) is used to find $\vec{J}^{\rm def}$ from Eqs. (16) and (12), where the components of $\vec{K}$ are

$$K_x=-\tfrac{1}{3}k_0,\quad K_y=0,\quad K_z=0\,, \tag{19}$$

for free electrons. The variable s is replaced by $k_\perp\phi$, where $k_\perp=k_0\sin\theta$, and k_0 is the radius of the Fermi sphere. The relation

$$e^{iz\sin\phi}=\sum_{n=-\infty}^{\infty}J_n(z)e^{in\phi} \tag{20}$$

can then be used to reduce the path integrals to sums of cylindrical Bessel functions. For the deformation force, Eq. (18) reduces to the following.

(I) For case $(\vec{i},\vec{k})$,

$$\Delta\epsilon^{\rm def}=\frac{iq\dot{u}\hbar^2k_0^2}{eB}\times\sum_{m,n}\frac{e^{i\phi(m-n)}}{ak_\perp+im}\times\left[\left[\frac{m^2}{X^2}-\frac{1}{3}\right]J_m-\frac{\sin\theta}{X}J_m'\right]J_n\,. \tag{21}$$

(II) For case $(\vec{j},\vec{k})$,

$$\Delta\epsilon^{\rm def}=\frac{q\dot{u}\hbar k_0^2}{eB}\sum_{m,n}\frac{e^{i\phi(m-n)}}{ak_\perp+im}\times(J_{m-2}-J_{m+2})\sin^2\theta J_n\,. \tag{22}$$

(III) For case $(\vec{k},\vec{k})$,

$$\Delta\epsilon^{\rm def}=\frac{iq\dot{u}\hbar^2k_0^2}{eB}\times\sum_{m,n}\frac{e^{i\phi(m-n)}}{ak_\perp+im}\times(J_{m-1}+J_{m+1})\sin\theta\cos\theta J_n\,. \tag{23}$$

The argument of the Bessel functions is $X\sin\theta$, where

$$X=qv_F/\omega_c=2\pi R/\lambda\,,$$

and R is the radius of the equatorial orbit.

Substitution of Eqs. (21)–(23) into Eq. (16) yields the components of the deformation currents for the following three cases.

(I) For case $(\vec{i},\vec{k})$,

$$J_x^{\rm def}=-ne\dot{u}\left[(1+i\omega\tau)\bar{\sigma}_{11}+\frac{q^2l^2}{3(1+i\omega\tau)}\bar{\sigma}_{11}-\omega_c\tau\bar{\sigma}_{12}-1\right], \quad (24)$$

$$J_y^{\rm def}=-ne\dot{u}\left[(1+i\omega\tau)\bar{\sigma}_{12}+\frac{q^2l^2}{3(1+i\omega\tau)}\bar{\sigma}_{12}+\omega_c\tau\bar{\sigma}_{22}\right], \quad (25)$$

$$J_z^{\rm def}=0 . \quad (26)$$

(II) For case $(\vec{j},\vec{k})$,

$$J_x^{\rm def}=-ne\dot{u}[(1+i\omega\tau)\bar{\sigma}_{12}+\omega_c\tau\bar{\sigma}_{11}] , \quad (27)$$

$$J_y^{\rm def}=-ne\dot{u}[(1+i\omega\tau)\bar{\sigma}_{22}-\omega_c\tau\bar{\sigma}_{12}-1] , \quad (28)$$

$$J_z^{\rm def}=0 . \quad (29)$$

(III) For case $(\vec{k},\vec{k})$,

$$J_x^{\rm def}=J_y^{\rm def}=0 , \quad (30)$$

$$J_z^{\rm def}=-ne\dot{u}[(1+i\omega\tau)\bar{\sigma}_{33}-1] . \quad (31)$$

In the expressions above n is the electron density and the $\bar{\sigma}_{ij}$ are the normalized components of the free-electron magnetoconductivity tensor for fields which vary as $e^{i(\omega t-qx)}$. They are the same as those given by CHH, with q and ω reversed in sign, but they have been divided by $\sigma_0=ne^2\tau/m$, where m is the electron mass.

Equations (24)–(31) can be substituted into Eq. (15) to find the self-consistent electric field and its contribution to the transient stress. The field components for the three cases are the following.

(I) For case $(\vec{i},\vec{k})$,

$$E_x=-\frac{m\dot{u}}{e\tau}\left[\bar{\rho}_{11}-(1+i\omega\tau)-\frac{q^2l^2}{3(1+i\omega\tau)}\right], \quad (32)$$

$$E_y=\frac{m\dot{u}}{e\tau}(\bar{\rho}_{12}-\omega_c\tau) , \quad (33)$$

$$E_z=0 . \quad (34)$$

(II) For case $(\vec{j},\vec{k})$,

$$E_x=-\frac{m\dot{u}}{e\tau}(\bar{\rho}_{12}-\omega_c\tau) , \quad (35)$$

$$E_y=-\frac{m\dot{u}}{e\tau}[\bar{\rho}_{22}-(1+i\omega\tau)] , \quad (36)$$

$$E_z=0 . \quad (37)$$

(III) For case $(\vec{k},\vec{k})$,

$$E_x=E_y=0 , \quad (38)$$

$$E_z=-\frac{m\dot{u}}{e\tau}[\bar{\rho}_{33}-(1+i\omega\tau)] . \quad (39)$$

The $\bar{\rho}_{ii}$, in terms of the σ_{ij}, are given by

$$\bar{\rho}_{11}=\frac{\sigma_0\sigma_{22}}{\sigma_{11}\sigma_{22}+\sigma_{12}^2} ,\quad \bar{\rho}_{22}=\frac{\sigma_0\sigma_{11}}{\sigma_{11}\sigma_{22}+\sigma_{12}^2} ,\quad \bar{\rho}_{33}=\frac{\sigma_0}{\sigma_{33}} . \quad (40)$$

The contribution of the self-consistent-field force to the transient stress $T^{\rm sc}$ is found from Eqs. (32)–(39), (18), and (11). In addition to causing the deformation current $\vec{J}^{\rm def}$ which leads to $T^{\rm sc}$, the deformation force Π also contributes directly to the transient stress an amount $T^{\rm def}$ which can be calculated by substituting Eq. (14) into Eq. (18), and then using the result in Eq. (11). Each of these contributions and their sums are given below for the three polarization conditions.

(I) For case $(\vec{i},\vec{k})$,

$$T^{\rm sc}=-\frac{in\dot{u}m}{q\tau}\left[\bar{\rho}_{11}-\omega_c^2\tau^2\bar{\sigma}_{22}-2(1+\omega_c\tau\bar{\sigma}_{12})\left[(1+i\omega\tau)+\frac{q^2l^2}{3(1+i\omega\tau)}\right]+\left[(1+i\omega\tau)+\frac{q^2l^2}{3(1+i\omega\tau)}\right]^2\bar{\sigma}_{11}\right], \quad (41)$$

$$T^{\rm def}=-\frac{in\dot{u}m}{q\tau}\left[\omega_c^2\tau^2\bar{\sigma}_{22}+(1+2\omega_c\tau\bar{\sigma}_{12})\left[(1+i\omega\tau)+\frac{q^2l^2}{3(1+i\omega\tau)}\right]-\left[(1+i\omega\tau)+\frac{q^2l^2}{3(1+i\omega\tau)}\right]^2\right], \quad (42)$$

$$T=T^{\rm sc}+T^{\rm def}=-\frac{in\dot{u}m}{q\tau}\left[\bar{\rho}_{11}-(1+i\omega\tau)-\frac{q^2l^2}{3(1+i\omega\tau)}\right]. \quad (43)$$

(II) For case $(\vec{j},\vec{k})$,

$$T^{sc}=-\frac{in\dot{u}m}{q\tau}[\bar{\rho}_{22}-2(1+i\omega\tau)-\omega_c^2\tau^2\bar{\sigma}_{11}+(1+i\omega\tau)^2\bar{\sigma}_{22}-2\omega_c\tau(1+i\omega\tau)\bar{\sigma}_{12}] , \tag{44}$$

$$T^{def}=-\frac{in\dot{u}m}{q\tau}[(1+i\omega\tau)+\omega_c^2\tau^2\bar{\sigma}_{11}-(1+i\omega\tau)^2\bar{\sigma}_{22}+2\omega_c\tau(1+i\omega\tau)\bar{\sigma}_{12}] , \tag{45}$$

$$T=-\frac{in\dot{u}m}{q\tau}[\bar{\rho}_{22}-(1+i\omega\tau)] . \tag{46}$$

(III) For case $(\vec{k},\vec{k})$,

$$T^{sc}=-\frac{in\dot{u}m}{q\tau}[\bar{\rho}_{33}-2(1+i\omega\tau)+(1+i\omega\tau)^2\bar{\sigma}_{33}] , \tag{47}$$

$$T^{def}=-\frac{in\dot{u}m}{q\tau}[(1+i\omega\tau)-(1+i\omega\tau)^2\bar{\sigma}_{33}] , \tag{48}$$

$$T=-\frac{in\dot{u}m}{q\tau}[\bar{\rho}_{33}-(1+i\omega\tau)] . \tag{49}$$

It is interesting to note that for each of the three cases the net transient stress is proportional to the self-consistent electric field in the direction of motion of the ions, i.e.,

$$T_{\vec{u}}=(ine/q)E_{\vec{u}} , \tag{50}$$

where $E_{\vec{u}}$ is $\vec{E}\cdot\vec{u}/u$, given by Eqs. (32), (36), and (39), respectively, for the three cases. Substitution of Eq. (50) into Eq. (4) yields

$$\rho\ddot{u}=-q^2\rho v_0^2 u+neE_{\vec{u}} . \tag{51}$$

Hence, in the moving reference frame the net force acting on the ions caused by the sound wave is just that due to the component of the self-consistent electric field in the direction of ion motion. The equivalent equation of motion in the laboratory frame contains an additional collision-drag term. It should further be noted that Eq. (19) in KP also reduces to our Eq. (51) for the free-electron model.

We now substitute the values found for $T_{\vec{u}}$ into Eqs. (9) and (10) to obtain the relative attenuation and dispersion, respectively,

$$\frac{\alpha_i}{q_i}=\frac{zm}{M\omega\tau}\left[\mathrm{Re}\bar{\rho}_{ii}-1-\frac{q_i^2l^2}{3(1+\omega^2\tau^2)}\delta_{i1}\right] , \tag{52}$$

$$\frac{\delta v_s}{v_{0i}}=-\frac{zm}{2M}\left[\frac{\mathrm{Im}\rho_{ii}}{\omega\tau}-1+\frac{q_i^2l^2}{3(1+\omega^2\tau^2)}\delta_{i1}\right] . \tag{53}$$

Here z is the valence and M the mass of the ions, and $i=1$, 2, or 3 for the three different polarization directions being considered.

The expressions for the attenuation are the same as those found by CHH in the laboratory reference frame. The expressions for the dispersion are the same as those of Rodriguez[3] under the approximation

$$\omega_c\tau/(1+i\omega\tau)\gg 1 .$$

They agree with the results of Chang and Gavenda[4] except for an unimportant static renormalization.

The normalized attenuation α_N and velocity v_N are plotted as functions of

$$X=ql/\omega_c\tau=2\pi R/\lambda$$

for case $(\vec{i},\vec{k})$ in Fig. 1 and cases $(\vec{j},\vec{k})$ and $(\vec{k},\vec{k})$ in Fig. 2, where

$$\alpha=(zm/Mv_0\tau)\alpha_N \tag{54}$$

and

$$\delta v_s/v_0=(zm/2M)v_N . \tag{55}$$

In these graphs $ql=100$ and $\omega\tau=1$, which means that $v_F/v_0=100$ and that $\omega=\omega_c$ for $X=100$.

The two kinds of oscillations in the curves can be related to two different kinds of resonance. The rapid oscillations come from geometric resonances which occur when the diameters of the electron orbit equal integral numbers of sound wavelengths. The slowly varying background is related to acoustic cyclotron resonance (ACR), which occurs when the acoustic frequency is some integral multiple of the electron cyclotron frequency . Of course, strong resonances are observed only for $\omega\tau>1$, but evidence of ACR is seen for $\omega\tau\approx 1$.

IV. ANALYTICAL EXPRESSIONS DERIVED FOR $D \gg \lambda$

The role played by ACR is more readily apparent from analytical expressions for the attenuation and velocity derived by taking the low-field limit ($X=D/\lambda \to \infty$). Asymptotic expressions for the conductivity tensor were given by Gavenda and Chang.[14] When substituted into Eqs. (52) and (53), they lead to the following.

(I) For case $(\vec{i},\vec{k})$,

$$\alpha_N \cong \frac{\pi q l}{6} \sinh\left[\frac{\pi X}{ql}\right] \frac{\cosh\left[\frac{\pi x}{ql}\right] + (\pi X)^{-1/2} \cos\left[\frac{\pi\omega}{\omega_c}\right] \sin\left[2X - \frac{\pi}{4}\right]}{\sinh^2\left[\frac{\pi X}{ql}\right] + \sin^2\left[\frac{\pi\omega}{\omega_c}\right]}, \tag{56}$$

$$v_n \cong \frac{\pi v_F}{6 v_0} \sin\left[\frac{\pi\omega}{\omega_c}\right] \frac{\cos\left[\frac{\pi\omega}{\omega_c}\right] + (\pi X)^{-1/2} \cosh\left[\frac{\pi X}{ql}\right] \sin\left[2X - \frac{\pi}{4}\right]}{\sinh^2\left[\frac{\pi X}{ql}\right] + \sin^2\left[\frac{\pi\omega}{\omega_c}\right]}. \tag{57}$$

(II) For case $(\vec{j},\vec{k})$,

$$\alpha_N \cong \frac{4ql}{3\pi} \sinh\left[\frac{\pi X}{ql}\right] \times \frac{\cosh\left[\frac{\pi X}{ql}\right] - 2(\pi X)^{-1/2} \cos\left[\frac{\pi\omega}{\omega_c}\right] \sin\left[2X - \frac{\pi}{4}\right]}{\sinh^2\left[\frac{\pi X}{ql}\right] + \cos^2\left[\frac{\pi\omega}{\omega_c}\right] - 4(\pi X)^{-1/2} \cosh\left[\frac{\pi X}{ql}\right] \cos\left[\frac{\pi\omega}{\omega_c}\right] \sin\left[2X - \frac{\pi}{4}\right] + 4(\pi X)^{-1} \sin^2\left[2X - \frac{\pi}{4}\right]}, \tag{58}$$

$$v_N \cong -\frac{4ql}{3\pi} \sin\left[\frac{\pi\omega}{\omega_c}\right] \times \frac{\cos\left[\frac{\pi\omega}{\omega_c}\right] - 2(\pi X)^{-1/2} \cosh\left[\frac{\pi X}{ql}\right] \sin\left[2X - \frac{\pi}{4}\right]}{\sinh^2\left[\frac{\pi X}{ql}\right] + \cos^2\left[\frac{\pi\omega}{\omega_c}\right] - 4(\pi X)^{-1/2} \cosh\left[\frac{\pi X}{ql}\right] \cos\left[\frac{\pi\omega}{\omega_c}\right] \sin\left[2X - \frac{\pi}{4}\right] + 4(\pi X)^{-1} \sin^2\left[2X - \frac{\pi}{4}\right]}. \tag{59}$$

(III) For case $(\vec{k},\vec{k})$,

$$\alpha_n \cong \frac{4ql}{3\pi} \left\{ \frac{\sinh\left[\frac{\pi X}{ql}\right] \cosh\left[\frac{\pi X}{ql}\right]}{\sinh^2\left[\frac{\pi x}{ql}\right] + \cos^2\left[\frac{\pi\omega}{\omega_c}\right]} \right\}, \tag{60}$$

$$v_n \cong -\frac{4ql}{3\pi} \left\{ \frac{\sin\left[\frac{\pi\omega}{\omega_c}\right] \cos\left[\frac{\pi\omega}{\omega_c}\right]}{\sinh^2\left[\frac{\pi X}{ql}\right] + \cos^2\left[\frac{\pi\omega}{\omega_c}\right]} \right\}. \tag{61}$$

In these equations the geometric oscillations are

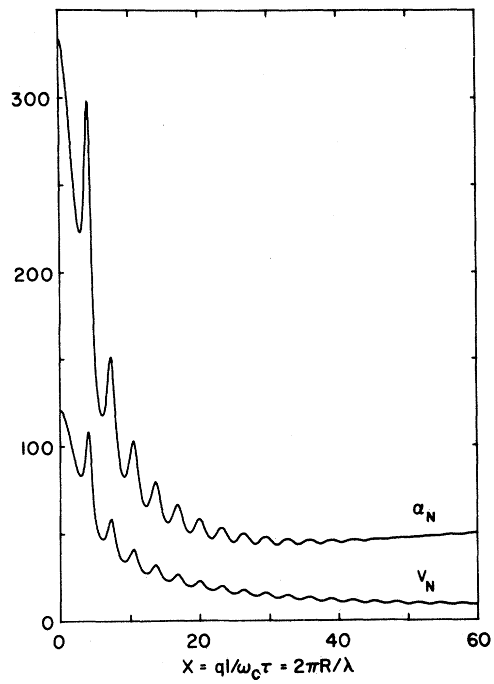

FIG. 1. Normalized attenuation α_N and velocity v_N for longitudinal waves propagating perpendicular to a magnetic field. Calculations are for a free-electron model with $ql=100$ and $\omega\tau=1$.

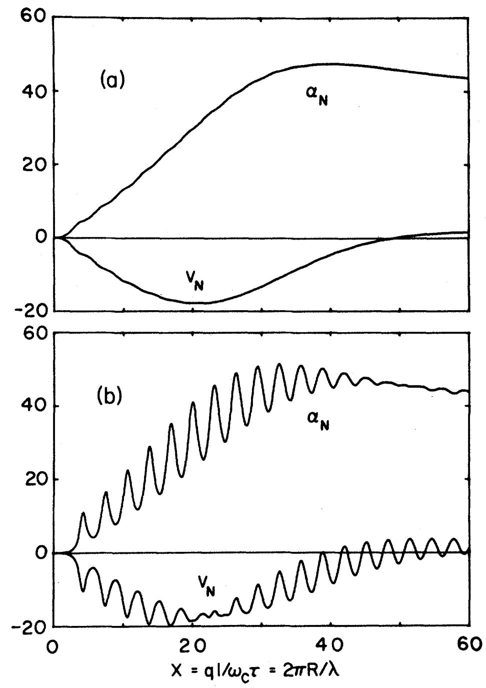

FIG. 2. Normalized attenuation α_N and velocity v_N for transverse waves propagating perpendicular to a magnetic field. Calculations are for a free-electron model with $ql=100$ and $\omega\tau=1$. (a) Polarization parallel to the field. (b) Polarization perpendicular to the field.

given by $\sin[2X-(\pi/4)]$. The ACR effects come from terms containing $\pi\omega/\omega_c$.

A reversal in the phase of geometric oscillations in the attenuation of compressional waves was first reported by Gavenda and Chang[15] in very pure Cd. They attributed it to the fact that for $\omega=\omega_c$ the sound field has moved a distance $\lambda/2$ while the electrons have gone halfway around their orbits. They thus encounter a field with the phase opposite that for smaller orbits (higher fields). In the free-electron calculation this effect is caused by the $\cos(\pi\omega/\omega_c)$ factor which multiplies the geometric oscillation term in the numerator of Eq. (56). The geometric oscillations vanish for $\omega_c=2\omega$, which occurs at $X=50$ in Fig. 1. The phase of the geometric oscillations in velocity depends on the $\sin(\pi\omega/\omega_c)$ factor in Eq. (57). The amplitude vanishes (and the phase reverses) at $\omega_c=\omega$, or $X=100$, for the parameters used in Fig. 1.

The geometric oscillations in the attenuation of shear waves polarized perpendicular to $\vec{B}$ [case $(\vec{j},\vec{k})$] show the same behavior as for compressional waves as can be seen in Fig. 2(b). This is not what one would expect at first glance from the asymptotic equations since the geometric term in the numerator of Eq. (58) has the opposite sign from the corresponding term in Eq. (56). However, it turns out that it is actually the third terms in the denominators of Eqs. (58) and (59) which cause the oscillations. The oscillations in velocity for case $(\vec{j},\vec{k})$ behave somewhat differently. For $X>25$, they have the same general behavior as in case $(\vec{i},\vec{k})$. For $X<25$, however, their phase is reversed. By varying the parameters we found that the phase reversal occurs when $\pi X/ql$ (which is equivalent to $\pi/\omega_c\tau$) is of order unity or less. Very few shear-velocity-shift measurements are available for comparison with these predictions. There is some evidence[16] for belly orbits in copper that a phase shift occurs in the predicted field range, but further experiments are needed to show this conclusively.

Finally, for shear waves polarized parallel to $\vec{B}$ we see in Fig. 2(a) that the geometric oscillations are extremely weak. This is basically due to the fact that the electron orbits which lead to geometric oscillations must have an oscillatory velocity component parallel to the ionic motion. For a spherical Fermi surface no such motion is present. It is interesting to note that the background behavior of the curves in Fig. 2(a) is identical with the curves in Fig. 2(b).

That is, the field-dependent attenuation and velocity for shear waves which arises from acoustic cyclotron resonance is independent of the wave polarization.

V. SUMMARY

We have shown how Pippard's deformation-coefficient theory for ultrasonic attenuation can be extended to yield dispersion as well. We find the attenuation and dispersion, in the case of free-electron metal, to agree with earlier calculations made in the laboratory reference frame. For this model, the effective force on the ions in the equation of motion turns out to be simply that of the self-consistent electric field.

A new result is that the phase of the geometric oscillations in velocity shifts by 180° relative to the oscillations in attenuation for $\omega_c \tau > \pi$. This can be seen from the asymptotic analytical expressions which we derive for the weak-field limit.

ACKNOWLEDGMENTS

We wish to thank Professor P. R. Antoniewicz for helpful discussions of the theory. This work was supported by the National Science Foundation under Grants Nos. DMR-76-11331 and DMR-78-25232.

*Present address: Motorola Semiconductor Group, Mesa, AZ 85202.

†Present address: Wright-Patterson Air Force Base, OH 45433.

[1]W. M. Theis and J. D. Gavenda, Phys. Rev. B 19, 3857 (1979).

[2]A. B. Pippard, Proc. R. Soc. London Ser. A 257, 165 (1960).

[3]S. Rodriguez, Phys. Rev. 132, 535 (1963).

[4]S. J. Chang and J. D. Gavenda, Phys. Rev. B 22, 1789 (1980).

[5]V. M. Kontorovich, Zh. Eksp. Teor. Fiz. 45, 1638 (1963) [Sov. Phys.—JETP 18, 1125 (1964)].

[6]V. G. Skobov and E. A. Kaner, Zh. Eksp. Teor. Fiz. 46, 273 (1964) [Sov. Phys.—JETP 19, 189 (1964)].

[7]J. Mertsching, Phys. Status Solidi 14, 3 (1966); 16, 267 (1966); 37, 465 (1970).

[8]L. P. Kadanoff and A. B. Pippard, Proc. R. Soc. London Ser. A 292, 299 (1966).

[9]L. D. Landau and E. M. Lifshitz, *Theory of Elasticity* (Addison-Wesley, Reading, Massachusetts, 1959), pp. 1—42, 98.

[10]A similar derivation of the dispersion relations in terms of the transient stress has been given by H. N. Spector, in *Solid State Physics,* edited by F. Seitz and D. Turnbull (Academic, New York, 1966), Vol. 19, p. 291, but he does not relate the transient-stress tensor to properties of the Fermi electrons in metals.

[11]R. G. Chambers, Proc. R. Soc. London Ser. A 65, 458 (1952).

[12]M. H. Cohen, M. J. Harrison, and W. A. Harrison, Phys. Rev. 117, 937 (1960).

[13]The assumption of perfect screening, made to simplify the calculations, breaks down at frequencies sufficiently high that the skin depth is no longer much smaller than the wavelength.

[14]J. D. Gavenda and F. H. S. Chang, Phys. Rev. 186, 630 (1969). The following corrections should be made: The right-hand side of Eq. (A1) should be multiplied by $(1-i\omega\tau)$, the first term on the right-hand side of Eq. (A12) should be multiplied by 2, and the right-hand side of Eq. (A23) should be divided by 4.

[15]J. D. Gavenda and F. H. S. Chang, Phys. Rev. Lett. 16, 228 (1966).

[16]C. M. Casteel, Ph.D. thesis, The University of Texas at Austin, 1978 (unpublished).